Radical reaction kinetics during homolysis of *N*-alkoxyamines: verification of the persistent radical effect

Thomas Kothe, Sylvain Marque, Rainer Martschke, Maxim Popov and Hanns Fischer *

Physikalisch-Chemisches Institut der Universität, Winterthurerstrasse 190, CH-8057 Zürich, Switzerland

N-Alkoxyamines cleave into transient alkyl and persistent aminoxyl radicals which then combine and regenerate the parent compounds. Simultaneously, the alkyl species self-terminate, and this causes a continuous build-up of excess aminoxyl. Hence, the back-reaction to the alkoxyamine accelerates and the self-termination slows down in time. An analysis of this self-regulating Persistent Radical Effect shows that in the absence of scavengers the alkoxyamines decay and the aminoxyls appear according to unusual $t^{1/3}$ rate laws governed by a rate constant combination. This is verified by studying the aminoxyl release from 2-phenyl-2-(2′,2′,6′,6′-tetramethylpiperidine-1′-oxyl)propane (cumyl–TEMPO). The rate constants of the individual reactions are also determined under isolation conditions and explain the behaviour of the combined reaction system. Mechanistic details of the reactions are given, and their relevance for 'living' radical polymerizations is pointed out.

N-Alkoxyamines are important initiators and intermediates in 'living' radical polymerizations which yield polymers with unusually low polydispersities, adjustable molecular weights and new block-copolymer architectures. Recently, this field has attracted extreme academic and industrial interest.[1] It is understood now that successful processes require a critical coupling of several reactions. These are the cleavage of the initiators and of intermediate alkoxyamine capped chains into propagating alkyl and persistent aminoxyl radicals, the reformation of the alkoxyamine capped chains by radical cross-coupling, the irreversible self-termination of the alkyl species and their addition to the monomer. In earlier work,[2] we have pointed out that the kinetics of polymerizations involving aminoxyl radicals or other persistent radicaloid species[3] are closely related to a general phenomenon which appears in reactions where transient and persistent radicals are formed simultaneously, the Persistent Radical Effect. It is characterized by a highly specific formation of the cross-reaction products of transient and persistent species and operates in diverse chemical systems.[4]

In order to explore the unusual kinetics associated with this effect in more detail we present here a kinetic analysis of the reactions involved in the thermal decay of alkoxyamines and prove the results with experiments on the homolysis of a prototype alkoxyamine, 2-phenyl-2-(2′,2′,6′,6′-tetramethylpiperidine-1′-oxyl)propane (cumyl–TEMPO) in an inert solvent.

As shown in Scheme 1, cumyl–TEMPO is expected to fragment into cumyl and TEMPO radicals [reaction (1), rate constant k_I]. Aminoxyl radicals scavenge alkyl and benzylic radicals effectively,[5] and, hence, the cross-coupling to the alkoxyamine [reaction (2)] has a high rate constant (k_x). TEMPO does not dimerize and is persistent in inert solvents even at elevated temperatures.[6] Thus, it is consumed in reaction (2) only. On the other hand, cumyl radicals disappear not only in reaction (2) but also in their close to diffusion controlled self-termination with rate constant $2k_t$. This occurs predominantly by combination to dicumyl but also to a minor extent (5–7%) by disproportionation to cumene and α-methylstyrene and by coupling to unstable semibenzenes.[7]

If the cleavage reaction (1) and the terminations (2) and (3) are the only kinetically relevant processes, the transient cumyl and the persistent TEMPO radicals appear at the onset of the
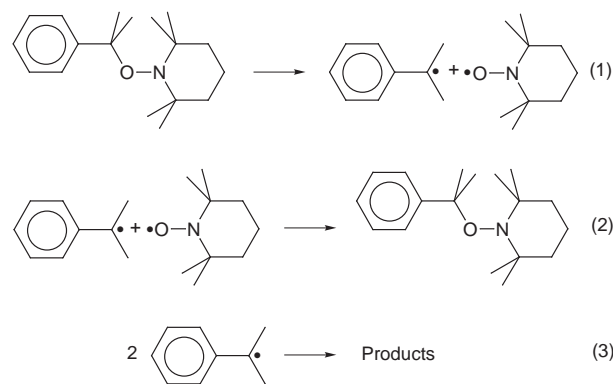

Scheme 1

process in equal concentrations. Thereafter, the terminations set in, and due to the self-termination the cumyl radicals disappear more effectively than the aminoxyl. This causes a continuous build-up of excess TEMPO which increases the rate of regeneration of the parent compound and diminishes the role of the self-termination as time proceeds. Consequently, the apparent decay rate of the alkoxyamine, the rate of TEMPO appearance and the self-termination rate slow down. Then, they will depend on a combination of all rate constants k_I, k_x and $2k_t$ and on the initial concentration.

In the following, we will first analyse these kinetics. We find that the concentrations of the radical species do not reach intermediate steady states but follow peculiar third root time dependences in realistic observation times. This is verified by EPR observation of the TEMPO appearance. To further prove the theoretical results, we also measure the rate constants and the activation parameters of the individual reactions under conditions of kinetic isolation. For reaction (1) the TEMPO appearance is monitored during the decay of the alkoxyamine in the presence of a large excess of the radical scavenger galvinoxyl.† The cross-reaction (2) is observed by kinetic absorption and chemically induced dynamic nuclear polarization (CIDNP)

---

† Galvinoxyl is 2,6-di-*tert*-butyl-4-(3,5-di-*tert*-butyl-4-oxocyclohexa-2,5-dien-1-ylidenemethyl)phenoxyl.

measurements of cumyl generated by flash photolysis from dicumyl ketone in the presence of TEMPO, and the self-termination (3) for cumyl is also observed by kinetic absorption spectroscopy. Finally, the combination of the individual rate constants is shown to lead to the observed TEMPO appearance in the combined system.

The particular alkoxyamine was chosen because it is easily prepared and purified, and the radicals are conveniently observed by EPR and absorption spectroscopy. However, besides the reactions (1) to (3) there is also a low fraction of disproportionation of cumyl and TEMPO to α-methylstyrene [reaction (4)]. This causes an irreversible removal of TEMPO and affects the kinetics especially at large conversions.

(4)
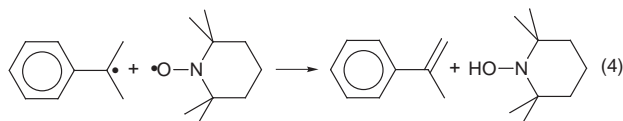
Reaction kinetics

In the following we denote the concentrations of the alkoxyamine by I, cumyl by R, TEMPO by Y and the cumyl groups in the self-termination products by P. Initially, all concentrations are zero except that of the alkoxyamine I_0. In the first stage, the disproportionation (4) is neglected. In this case the material balance of TEMPO and cumyl groups requires $Y = I_0 - I$ and $P = Y - R$ at all times. Hence, one has to solve the kinetic equations for two dependent variables, only, for which R and Y are a natural choice. These are given in eqns. (5)

$$\frac{dR}{dt} = k_I I - k_x RY - 2k_t R^2 = k_I I_0 - k_I Y - k_x RY - 2k_t R^2 \quad (5)$$

and (6) and have no closed analytical solution. Approximations

$$\frac{dY}{dt} = k_I I - k_x RY = k_I I_0 - k_I Y - k_x RY \quad (6)$$

for the special case of $k_x = 2k_t$ were found previously.[2] Here, this restriction is removed, *i.e.* more realistic solutions are obtained.

Before presenting these solutions, we note that in contrast to usual radical chemistry neither the transient species R nor the aminoxyl radical Y can be treated with intermediate steady state or quasi-steady state approximations. Setting the time derivatives of R and Y in eqns. (5) and (6) to zero yields immediately $R_S = 0$ and $Y_S = I_0$. Thus, only at the end of the reactions is a steady state approached when the alkoxyamine is fully converted to aminoxyl and cumyl containing products.

At the beginning of the process and as long as R and Y are still very small, both radical concentrations increase linearly with time [eqn. (7)]. Together with the behaviour at long times

$$R = Y = k_I I_0 t \quad (7)$$

this means that Y must increase monotonically, and that $R(t)$ has an intermediate maximum. By inserting eqn. (7) into eqn. (5) and setting the time derivative to zero the maximum is found at approximately $\hat{t}$ [eqn. (8)], which is in the millisecond region

$$\hat{t} = [k_I I_0 (k_x + 2k_t)]^{-1/2} \quad (8)$$

for reasonable parameters (*vide infra*). There, R attains a value of about 10^{-7} M which is hardly observable. Further, at very long times when Y has reached the steady state, the concentration of the transient R decays proportionally to $1/t$.

To find an approximate solution for the intermediate time range, we cast the two non-linear first-order eqns. (5) and (6)
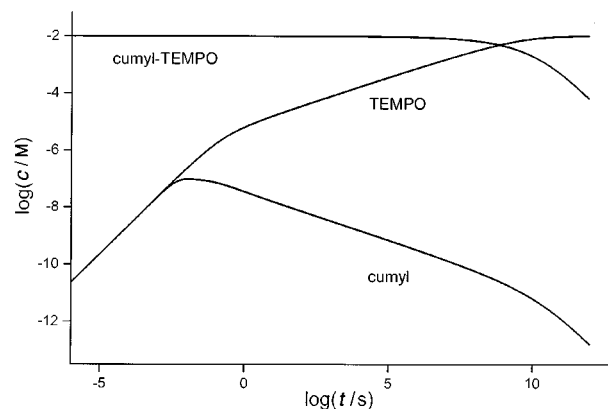
Fig. 1 Numerically calculated time dependencies of concentrations in double logarithmic presentation

into one non-linear second-order equation for Y, only, and use the expression $Y = CI_0\tau^n$ with a dimensionless time variable $\tau = k_I t$. The power dependence on time is suggested by the behaviour at short and long times. Further, the monotonically slowing down evolution of Y requires $0 \leqslant n \leqslant 1$. With the abbreviations $a = k_x I_0/k_I$ and $b = 2k_t I_0/k_I$ one finds a time invariant expression [eqn. (9)]. The individual terms on the left hand

$$Cn[2 + a/b - C(n + a/b)\tau^{n-1}]\tau^{n-1} + (C^3 na^2/b\tau^{3n-1}) - 2C^2 n\tau^{2n-1} + C(2 - C\tau^n)\tau^n = 1 \quad (9)$$

side of eqn. (9) become time independent for different values of n and form the desired approximate solutions if the other terms are negligible.

The first term leads to $n = 1$ and $C = 1$ and gives directly the short time solution (7). The last term is time independent for $n = 0$, gives again $C = 1$, and the long time limit $Y = I_0$. The third term is negative and does not provide a physically meaningful result. Finally, the second term yields[8] $n = 1/3$ and $C^3 = 3b/a^2$ which translates into eqn. (10). Insertion of eqn. (10) into eqn.

$$Y = I_0^{2/3}(3k_I^2 2k_t/k_x^2)^{1/3} t^{1/3} \quad (10)$$

(6) then shows that R is approximately given by eqn. (11). With

$$R = I_0^{1/3}(k_I/3k_x 2k_t)^{1/3} t^{-1/3} \quad (11)$$

Y and R known the concentrations I and P follow from the material balance equations. From the condition that the other terms in eqn. (9) must be small one obtains the range of validity of eqns. (10) and (11), given in eqn. (12).

$$(2k_t/k_I I_0)^{1/2}(2 + k_x/2k_t)^{3/2}/3k_x \ll t \ll k_x^2 I_0/24k_I^2 2k_t \quad (12)$$

For many realistic cases and observation times the unusual third root solutions in eqns. (10) and (11) should hold rather well. Insertion of the parameters observed below for the thermolysis of cumyl–TEMPO in *tert*-butylbenzene at 83 °C ($I_0 = 10$ mM, $k_I = 2.3 \times 10^{-3}$ s^{-1}, $k_x = 9.1 \times 10^7$ M^{-1} s^{-1}, $2k_t = 2.3 \times 10^9$ M^{-1} s^{-1}) into the inequality (12) leads to a lower time border of 100 ms and an upper border of 1.5×10^7 s = 4200 h. At these times cumyl–TEMPO is decomposed to 0.035 and 19%, respectively. The upper border demonstrates that the decay of cumyl–TEMPO is strongly delayed by the Persistent Radical Effect. In its absence the natural lifetime would be $k_I^{-1} = 435$ s, only.

Fig. 1 shows the results of a numerical solution of the kinetic equations (5), (6) with the parameters given above. In this double logarithmic plot the initial ($t < 1$ s), intermediate (1 s $< t < 10^7$ s) and final ($t > 10^7$ s) time ranges are clearly separated. In Fig. 2 we compare the evolution of TEMPO in
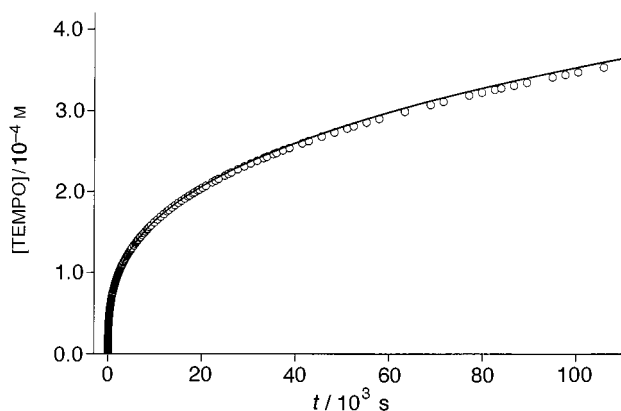
Fig. 2 Calculated time dependence of the TEMPO concentration. Circles from the numerical calculation as in Fig. 1, line from eqn. (10), for parameters see text.
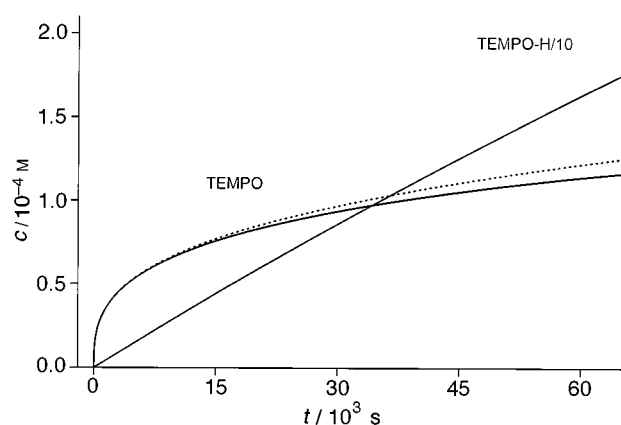

Fig. 3 Calculated time dependencies of TEMPO and TEMPO-H including 0.5% disproportionation reaction (4). Dotted line without disproportionation. $k_I = 7 \times 10^{-4}$ s^{-1}, other parameters see text.

the intermediate time range up to about 30 h as calculated numerically (circles) and from eqn. (10) (solid line). The agreement between the more exact numerical and the approximate $t^{1/3}$ solution is gratifying. Since TEMPO has to reach a finite final concentration there are deviations at long times. These are noticeable although in the considered time range the conversion is below 4%.

In 'living' radical polymerizations[1,3] it is often assumed that the transient and the persistent species are in equilibrium with their precursor. Multiplication of eqns. (10) and (11) gives eqn. (13). Obviously, in the intermediate time range and for low

$$k_x RY = k_I I_0 \qquad (13)$$

alkoxyamine conversion, reactions (1) and (2) are in equilibrium, and this is expected to be also valid in 'living' polymerizations. However, eqn. (13) is not the law of mass action in the usual sense, since the radical concentrations R and Y are time dependent. Yet, the time dependence cancels out.

For cases with considerable disproportionation [reaction (4)] we have not yet found an analytical solution. However, for small conversions the rate of disproportionation follows from eqn. (13) as $f_D k_x RY = f_D k_I I_0$, where f_D is the fraction of disproportionation. The concentrations of the disproportionation products thus increase linearly with time. Even for small fractions f_D they will dominate the self-termination products P because $f_D k_x RY/2k_t R^2$ becomes large as Y/R increases constantly. For large conversions, the release of TEMPO is diminished, and its concentration does not reach I_0. These features are confirmed by numerical calculations using the parameters given before (Fig. 3).
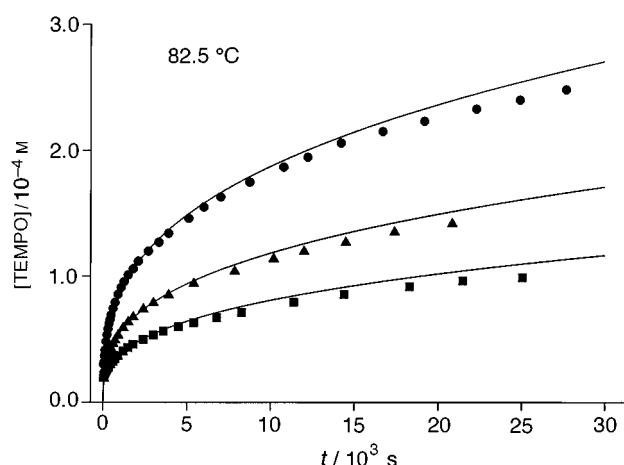

Fig. 4 Time dependence of the TEMPO concentration during thermolysis of cumyl–TEMPO: ●, 1.16×10^{-2} M; ▲, 5.10×10^{-3} M; ■, 2.52×10^{-3} M

Concluding this section we point out again that it is not possible to extract individual rate constants directly from the apparent decay of the radical precursor nor from the rate of radical formation in the intermediate time range. According to eqns. (10) and (11) these are governed by a combination of rate constants.

Experimental

2-Phenyl-2-(2′,2′,6′,6′-tetramethylpiperidine-1′-oxyl)propane (cumyl–TEMPO) was synthesized following ref. 9a, repeatedly recrystallized (ethanol–hexane 3:1), dried, stored at −20 °C, and had a purity of at least 98% (NMR). Dicumyl ketone (>97%) was prepared by a conventional method.[9b] TEMPO (Aldrich) was sublimed and found to be 97% pure by titration.[10a] Galvinoxyl (Aldrich) was used as received (purity 96% by titration,[10a] mp 158.5 °C, lit. 157.5 °C[10b]). The solvent *tert*-butylbenzene was carefully purified by standard procedures and stored under nitrogen.

Time evolutions of radical concentrations were followed by continuous wave (CW)–EPR spectroscopy (Bruker ER 100E) with samples prepared shortly before use, deoxygenated by several freeze–pump–thaw cycles and sealed under helium. Standard samples with known persistent radical concentrations served for calibrations. The radical concentrations were kept low to avoid spin exchange line broadening effects. Time resolved absorption spectroscopy following 308 nm laser flash photolysis of dicumyl ketone employed an apparatus described earlier[11] and a flow system with solutions freed from oxygen by argon purging. The instrumentation and the procedures for time resolved 200 MHz ^{1}H CIDNP studies after laser flash initiation have also been described.[12] Product analysis involved NMR and GLC. In all experiments with slow TEMPO formation extreme cleaning and preconditioning of the glassware was essential to obtain reproducible results.

Results and discussion

TEMPO evolution during homolysis of 2-phenyl-2-(2′,2′,6′,6′-tetramethylpiperidine-1′-oxyl)propane (cumyl–TEMPO)

Fig. 4 shows the appearance of TEMPO measured by CW–EPR during thermolysis of cumyl–TEMPO in *tert*-butylbenzene at 82.5 °C for three initial concentrations over a period of about 8 h which leads to about 2% conversion. The same data are plotted against $t^{1/3}$ in Fig. 5 as suggested by eqn. (10). Apart from distortions at very early times which are due to effects of thermal equilibration the data confirm the predicted behaviour. At long times the $t^{1/3}$ rate law should be only approximate (Fig. 2). Therefore, only the initial slopes of the
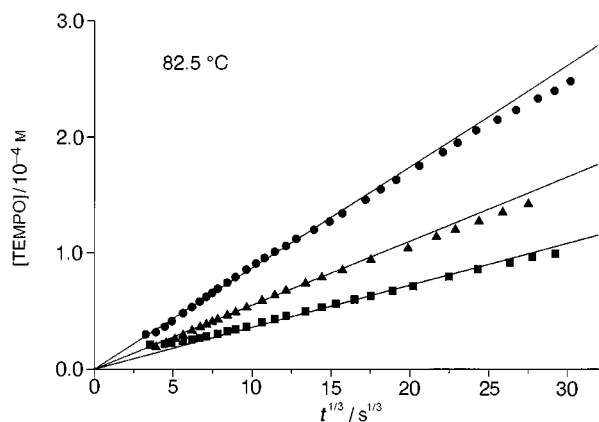
Fig. 5 Time dependence of the TEMPO concentration during thermolysis of cumyl–TEMPO plotted *vs.* $t^{1/3}$: ●, 1.16×10^{-2} M; ▲, 5.10×10^{-3} M; ■, 2.52×10^{-3} M
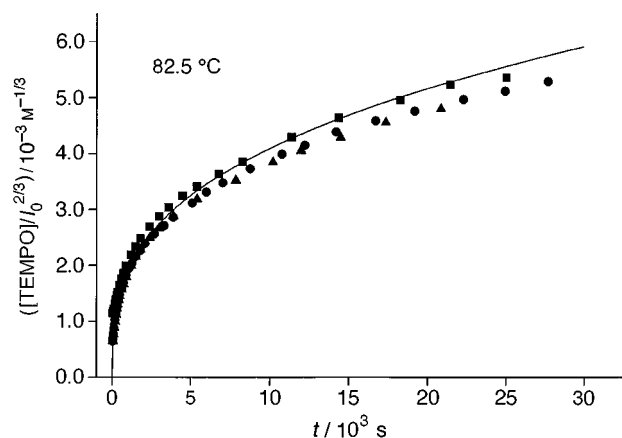

Fig. 6 Time dependence of the reduced TEMPO concentrations during thermolysis of cumyl–TEMPO (symbols as in Fig. 4)

Fig. 7 Temperature dependence of the rate parameter $3k_{\mathrm{I}}^2 2k_t/k_x^2$

Fig. 8 Time dependence of the TEMPO concentration during thermolysis of cumyl–TEMPO in a 25-fold excess of galvinoxyl

data of Fig. 5 were inserted into eqn. (10) to obtain the solid lines. Yet, the long time deviations are larger than predicted by Fig. 2, and this is very probably due to the disproportionation of cumyl and TEMPO to α-methylstyrene and TEMPO-H [*cf.* reaction (4) and Fig. 3]. Extension of the measurements to longer times only gave satisfactory results in a few cases. Often, the time dependence changed irreproducibly, probably because of interfering reactions with remaining impurities.

According to eqn. (10) the slopes of the lines in the plot *vs.* $t^{1/3}$ should depend on the initial cumyl–TEMPO concentration as $I_0^{2/3}$. The observed data support this strongly as shown in Fig. 6 for the time evolution of the appropriately reduced TEMPO concentrations.

Experiments in the range of 65 to 93 °C provided similar results though at higher temperatures the long time deviations from the $t^{1/3}$ prediction were more expressed. From the slopes of the $t^{1/3}$ plots at early times, the TEMPO appearance constant $3k_{\mathrm{I}}^2 2k_t/k_x^2$ [eqn. (10)] was determined. The results of 11 measurements at various temperatures are shown in Fig. 7 and give eqn. (14) (E_a in kJ mol^{-1}).

$$\log [(3k_{\mathrm{I}}^2 2k_t/k_x^2)/\mathrm{M\ s}^{-1}] =$$
$$22.3 \pm 0.4 - (228 \pm 3)/2.303RT \quad (14)$$

For the determination of the thermolysis products, 8–9 mM cumyl–TEMPO solutions in heptane or octane were deoxygenated, sealed in carefully cleaned NMR quartz sample tubes, thermostatted for 3 to 17.5 h at 80 °C and analysed immediately thereafter. For an initial concentration of 8.7 mM the typical product distribution was, after 17.5 h, 0.2 mM TEMPO, 0.05 mM dicumyl, 1.8 mM α-methylstyrene, 1.7 mM hydroxylamine
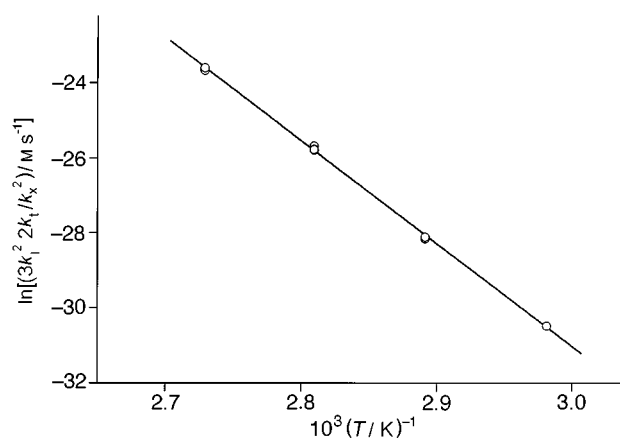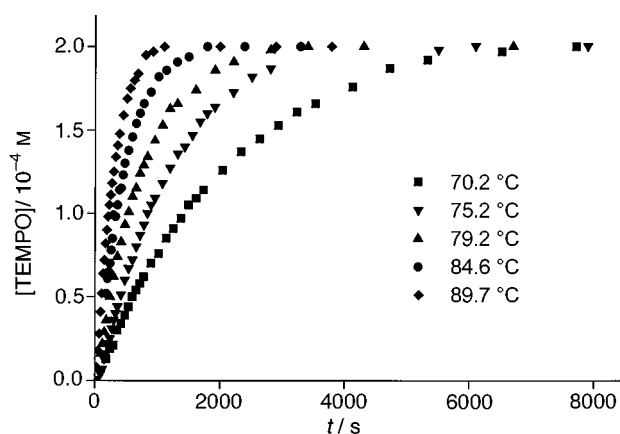
(TEMPO-H) and no other detectable species. As expected from Fig. 3, the concentrations of TEMPO-H and α-methylstyrene increased approximately linearly with time while the other products showed a weaker increase.

According to Scheme 1 the yield of TEMPO should be twice that of dicumyl. Yet, an excess of 0.1 mM is found because TEMPO is released from unreacted alkoxyamine on the GLC column. The formation of α-methylstyrene and TEMPO-H is clear evidence for the partial disproportionation [reaction (4)]. However, despite the relatively high yield this reaction does not compete effectively with the combination reaction (2). In fact, a simulation with $k_{\mathrm{I}} = 7 \times 10^{-4}$ s^{-1} at the lower temperature with the low fraction of disproportionation $f_D = 0.5\%$ gave, for 17.5 h thermolysis, 0.114 mM TEMPO, 0.055 mM dicumyl, 1.69 mM TEMPO-H and α-methylstyrene in agreement with the observed values. The calculated concentration *vs.* time profiles for this case have already been given in Fig. 3.

TEMPO evolution during homolysis of 2-phenyl-2-(2′,2′,6′,6′-tetramethylpiperidine-1′-oxyl)propane (cumyl–TEMPO) in the presence of galvinoxyl

To isolate reaction (1), *i.e.* to observe the decay of cumyl–TEMPO in the absence of the back reaction (2), the appearance of TEMPO was followed in *tert*-butylbenzene solutions containing initially 0.2 mM cumyl–TEMPO and the stable radical galvinoxyl in a large excess of 5 mM. In this case all cumyl radicals are expected to be scavenged by galvinoxyl. The EPR spectrum of galvinoxyl has an overall extension of about 15 G, and its centre is displaced by about 17 G from the low field line of TEMPO. Hence, TEMPO could be observed without overlap distortions in spite of the much higher galvinoxyl concentrations. Fig. 8 shows the time dependence of the TEMPO concentration at different temperatures. It reaches a saturation
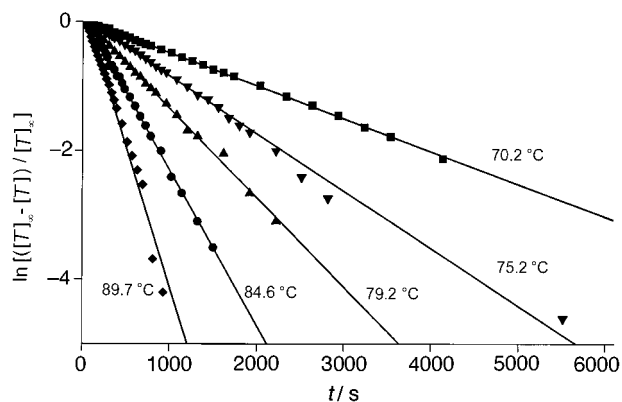
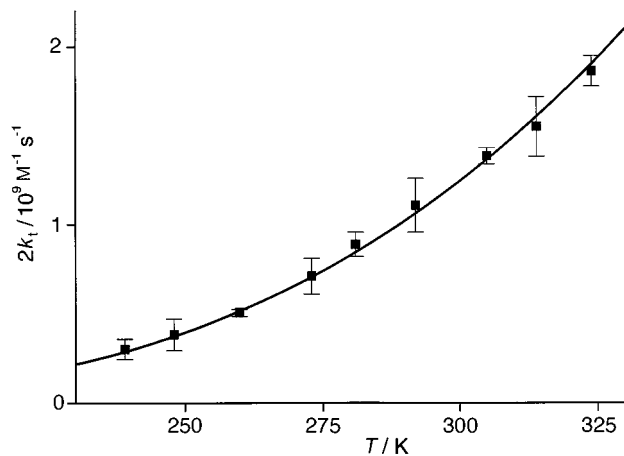**Fig. 9** First-order plot of the data given in Fig. 8

Fig. 10 Temperature dependence of the self-termination constant of cumyl radicals

Fig. 11 Temperature dependence of the cross-termination constant of cumyl and TEMPO

at 0.2 mM, *i.e.* the expected concentration for 100% conversion, and in times which are much shorter than those observed in the absence of the scavenger and for much smaller conversions (Fig. 4). Also, the shapes of the curves are quite different from those in Fig. 4. They are very well represented by first-order processes, and the decay rate constants follow from the corresponding plots of Fig. 9.

Similar results were obtained for other initial cumyl–TEMPO concentrations. However, for concentrations larger than 0.5 mM lower rate constants were found. This indicates that the released TEMPO then starts to compete with the scavenging galvinoxyl, and that the rate constant for the reaction of cumyl with galvinoxyl is not larger than k_x. For the lowest concentration ratios 1:25, 1:50 and 1:100 the decay constants reached a maximum limiting value which is attributed to the isolated reaction (1). In Arrhenius form (E_a in kJ mol^{-1}) the decay constants are given by eqn. (15). Reassuringly, the high

$$\log (k_I/s^{-1}) = 14.1 \pm 0.1 - (114.4 \pm 0.1)/2.303RT \quad (15)$$

frequency factor is typical for a cleavage reaction into large groups.

NMR experiments with C_6D_6 solutions of 2 mM cumyl–TEMPO and 2.5 mM galvinoxyl at 70 to 75 °C revealed the formation of α-methylstyrene and galvinol in a 1:1 ratio and in about 85% yields. Dicumyl and TEMPO-H were absent, so that reactions (3) and (4), and (2) by analogy, are in fact completely suppressed. The disproportionation of cumyl and galvinoxyl may be the major reaction now but the combination to an ether and its subsequent decomposition are more likely (*vide infra*). GLC experiments on the decomposition of 0.5 mM cumyl–TEMPO in benzene solutions containing 5 and 1 mM galvinoxyl revealed 0.5 mM α-methylstyrene and 0.5 mM TEMPO as products, no dicumyl and only traces of the hydroxylamine, again in full agreement with a complete cumyl scavenging.

Time resolved studies of the cumyl self- and cross-termination rate constants

Laser flash photolysis of dicumyl ketone (α,α,α′,α′-tetramethyldibenzyl ketone) at 308 nm provides a convenient, clean and instantaneous source of cumyl radicals because above 250 K the intermediate dimethylphenylacetyl radicals decarbonylate completely within 10 ns.[12b] To measure the self-termination rate constant 0.02 M ketone solutions in *tert*-butylbenzene were used, and the radical decay was monitored at the absorption maximum of 323 nm. From 240 to 325 K it followed a clean second-order rate law with lifetimes of 10 to 20 μs. The absorption coefficient was estimated from the ketone conversion as (4500 ± 1500) M^{-1} cm^{-1} and agrees with other data.[13] Using the average value, the rate constants (Fig. 10) are given by eqn. (16),

$$\log (2k_t/M^{-1} s^{-1}) = 11.6 \pm 0.1 - (14.3 \pm 0.2)/2.303RT \quad (16)$$

with E_a in kJ mol^{-1}. The frequency factor, the activation energy
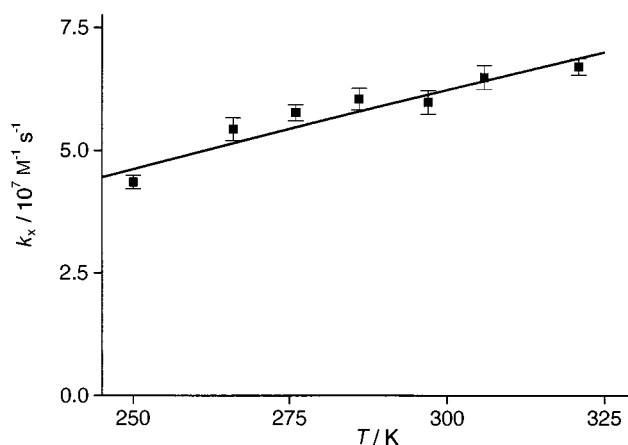
and the rate constants (2×10^8 to 2×10^9 M^{-1} s^{-1}) indicate that the self-termination occurs close to the diffusion controlled limit.

The isolated rate constant k_x for the cross-reaction (2) was determined from the decay of cumyl in the presence of 5 to 16 mM TEMPO following the lines of ref. 5. From 250 to 325 K TEMPO caused a clean pseudo-first-order decay of cumyl with a μs lifetime, and on this timescale cumyl–TEMPO is stable. In accord with earlier findings on the reaction of benzyl and other alkyl radicals with TEMPO,[5] k_x varied only little with temperature (Fig. 11, 4.3×10^7 to 6.7×10^7 M^{-1} s^{-1}) and is given by eqn. (17), with E_a in kJ mol^{-1}. The room temperature value

$$\log (k_x/M^{-1} s^{-1}) = 8.4 \pm 0.1 - (3.7 \pm 0.3)/2.303RT \quad (17)$$

$k_x = 6.0 \times 10^7$ M^{-1} s^{-1} is compatible with $k_x = 11.8 \times 10^7$ M^{-1} s^{-1} found earlier for isooctane solvent,[5a] since the cross-coupling constant is remarkably solvent dependent.[5] The rate constants are lower than diffusion controlled, and have a low frequency factor. Interpretations of these features have been offered.[5]

To further clarify the reaction between cumyl and TEMPO, time resolved CIDNP experiments were performed at room temperature. Fig. 12 shows the polarizations of the reaction products formed after 308 nm laser photolysis of [²H₈]toluene solutions containing 3 mM dicumyl ketone and 10.9 mM TEMPO. Most of the signals have been found earlier in the absence of TEMPO[12b] and are due to geminate reactions of the primary cumyl–dimethylphenylacetyl radical pairs (dicumyl ketone, 1.453 ppm, s; dicumyl, 1.416 ppm, s; α-methylstyrene, 2.18 ppm, q; aldehyde, 9.43 ppm, s). They all appear in enhanced absorption, and their intensities do not depend on the
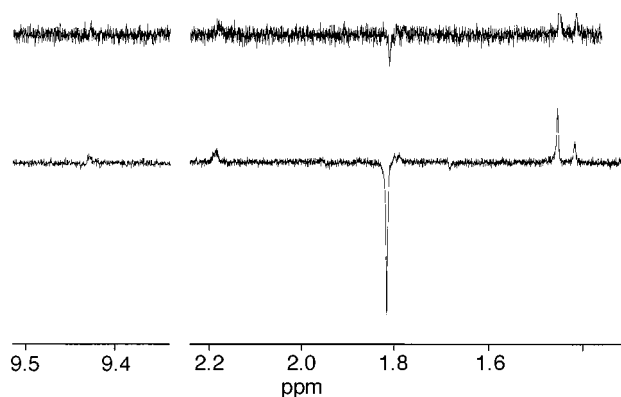
Fig. 12 Time resolved CIDNP spectra of products during the reaction of cumyl radicals with TEMPO. Upper trace 1 μs, lower trace 1000 μs after the laser flash.
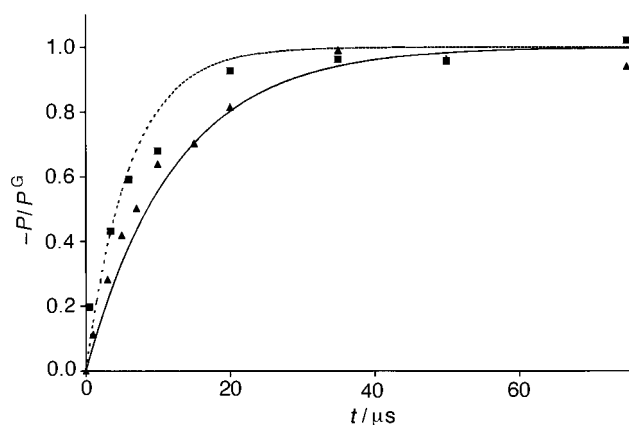

Fig. 13 Time evolution of the polarization of cumyl–TEMPO: ▲, 0.86 mM; ■, 1.73 mM

time delay between laser and NMR detection pulse. The new peak at 1.818 ppm belongs to the methyl groups of cumyl–TEMPO, is in emission and increases with time. This is caused by the transfer of the emissive polarization of cumyl radicals escaping the geminate process to the combination product. If the disproportionation to TEMPO-H and α-methylstyrene were important, the sign of the resonance at 2.18 ppm should turn to emission, but it does not exhibit a noticeable time dependence. From the limits of detection, the fraction of disproportionation must be below about 1%, in full agreement with our earlier conclusion of 0.5% from the product yields.

Fig. 13 displays the formation kinetics of the cumyl–TEMPO polarization measured for two TEMPO concentrations relative to the geminate polarization P^G after photolysis of 0.72 mM dicumyl ketone in [$^2H_8$]toluene. The final value of $-P/P^G = 1$ proves that the initial radical polarization is completely converted to the product. This re-ensures the absence of unknown side reactions and little nuclear relaxation of the cumyl species. It means further that the cross-reaction (2) leads to little extra polarization. To check this point cumyl–TEMPO was also photolysed directly in [$^2H_8$]propan-2-ol at 266 nm. As for benzyl–TEMPO[14] a direct singlet cleavage to cumyl and TEMPO was found with a low geminate polarization of cumyl–TEMPO of about $P^G = -10^{-4}$ per radical pair. In contrast, for the photolysis of dicumyl ketone the geminate polarization is about $P^G = 10^{-3}$ per radical pair, *i.e.* it is much larger and dominates in Fig. 12. Further, the direct photolysis of the alkoxyamine did not only lead to C–O but also to some O–N bond cleavage which was not considered in Scaiano's earlier work.[14]

For the ketone system the complete transfer of the polarization to the coupling product allows a simple analysis of the time dependence in terms of a pseudo-first-order cumyl scav-

enging similar to earlier analyses for addition and hydrogen atom transfer reactions.[15] The two lines in Fig. 13 are the corresponding fits to the data. They lead to $k_x = 9.5 \times 10^7$ M^{-1} s^{-1} in toluene at room temperature whereas $k_x = 6.0 \times 10^7$ M^{-1} s^{-1} was obtained in *tert*-butylbenzene by optical spectroscopy.

Finally, the scavenging of cumyl by galvinoxyl in [$^2H_8$]toluene was also followed by time resolved CIDNP. It led to an emissive singlet at 1.48 ppm which increased with time and is likely to belong to the coupling product of cumyl and galvinoxyl. However, this compound was not stable for long times and fragments probably into α-methylstyrene and galvinol which were observed as stable products.

Evaluation of the reaction rates and relations to controlled radical polymerization

From the rate constants of the isolated reactions (15)–(17) the rate parameter (14) entering the behaviour of the combined system is calculated as given in eqn. (18). The agreement with

$$\log [(3k_I^2 2k_t/k_x^2)/\text{M s}^{-1}] = $$
$$23.5 \pm 0.5 - (236 \pm 1.4)/2.303RT \quad (18)$$

the experimental relation (14) is very reasonable, and the small differences may partly be due to the uncertainty of the cumyl absorption coefficient.

The individual rate constants also yield the equilibrium constant of the cleavage of cumyl–TEMPO [eqn. (19)]. The

$$\log (K/\text{M}) = k_I/k_x = 5.7 \pm 0.2 - (110.4 \pm 0.6)/2.303RT \quad (19)$$

reaction entropy of $\Delta S = 109$ kJ mol^{-1} K^{-1} is large but usual for a fragmentation into large groups, and the reaction enthalpy $\Delta H = 110$ kJ mol^{-1} is the low C–O bond dissociation energy of cumyl–TEMPO. For an alkoxyamine cleaving reversibly to the persistent 1,1-diphenylethyl radical and 4-oxo-TEMPO, Howard[16] found $\Delta S = 150$ J mol^{-1} K^{-1} and $\Delta H = 90$ kJ mol^{-1}. The differences to cumyl–TEMPO are as expected since the 1,1-diphenylethyl species has a higher steric demand and is more stabilized.

In the field of 'living' radical polymerization various attempts have been made to obtain rate constants and mechanisms for the reactions of alkoxyamine initiators and of intermediate aminoxyl capped polymer chains. Several studies reveal the operation of the Persistent Radical Effect though this went unnoticed, until now. Thus, Priddy and co-workers[17] followed the decay of 1-phenyl-1-(2′,2′,6′,6′-tetramethylpiperidine-1′-oxyl)ethane (phenylethyl–TEMPO) in neat trichlorobenzene at 140 °C and found a half-life of about 2.5 h. On the contrary, for the same compound Hawker *et al.*[18] reported a half-life of only several minutes at 123 °C in styrene solution. Obviously, in the first case the decay is strongly subject to the Persistent Radical Effect. In the second, the 1-phenylethyl radicals are at least partly scavenged by addition to styrene so that a better approximation of the true cleavage reaction was obtained. Similar to our product distribution, Priddy *et al.*[17] observed styrene and the TEMPO-H as major and 1,2-diphenylbutane as minor products. To explain the major products they invoked an effective disproportionation of the primary alkyl–aminoxyl radical pair. This process was also assumed by Fukuda *et al.*[19] for the decay of TEMPO capped polystyrene. It is very unlikely because there is no disproportionation between cumyl and TEMPO under our radical scavenging conditions. Moreover, as shown above, the Persistent Radical Effect explains how a minor reaction between a transient and a persistent radical can lead to the majority of products, and an illuminating example for this behaviour is also found in Finke's work.[4d]

Furthermore, during 'living' styrene polymerization the evolution of TEMPO from polystyryl–TEMPO was observed by EPR.[20] Here, the self-initiation of styrene plays an important role and may obscure the $t^{1/3}$ dependence,[2] but it is gratifying to

note that the concentration increase is persistent and resembles our Fig. 4. In atom transfer polymerizations involving halide transfer to Cu^I, a paramagnetic Cu^{II} complex is the persistent radicaloid species, and its concentration also increases slowly during the reaction.[21]

Determinations of the rate constant k_I for the alkoxyamine cleavage under conditions of kinetic isolation are also available. Moad and Rizzardo[22] measured the disappearance of several alkoxyamines in the presence of an excess foreign aminoxyl by chromatography. For TEMPO capped poly-α-methylstyrene they reported a half-life of 10 min at 60 °C. Cumyl–TEMPO is a reasonable model for this compound though it is expected to decay slower for steric reasons, and eqn. (15) yields $t_{1/2}$ = 77 min at 60 °C. By chromatography, Goto *et al.*[23] observed the decay of a monodisperse polystyryl–TEMPO in the presence of styrene and of an additional initiator. The decay was exponential and led to log (k_I/s^{-1}) = 13.5 − 124/2.303RT, with E_a in kJ mol^{-1}. This is not far from our result for cumyl–TEMPO [eqn. (15)] but the frequency factor appears a little low. From the reported conditions it is not clear whether the isolation was complete, and, therefore, the rate constants may be slightly too low. Finally, semiempirical calculations on the bond dissociation energy have been carried out.[22,24] For 1-phenylethyl–TEMPO AM1 gave 92 kJ mol^{-1} and PM3 lead to 109 kJ mol^{-1}.[24] Cumyl–TEMPO should have a lower dissociation energy but we find 110 kJ mol^{-1}. Hence, the calculated values are probably too low estimates.

In summary, the results of this work confirm the unusual kinetics associated with the Persistent Radical Effect. They agree with many findings on mechanisms involved in aminoxyl and alkoxyamine mediated 'living' polymerizations and lead to their better understanding.

Acknowledgements

References

1 (*a*) D. H. Solomon, E. Rizzardo and P. Cacioli, US Patent, 1986, 4 581 429; (*b*) M. K. Georges, R. P. N. Veregin, P. M. Kazmaier and G. K. Hamer, *Macromolecules*, 1993, **26**, 2987; (*c*) D. Greszta and K. Matyjaszewski, *Macromolecules*, 1996, **29**, 7661; (*d*) C. J. Hawker, J. L. Hedrick, E. E. Malmström, M. Trollsas, D. Mecerreyes, G. Moineau, P. Dubois and R. Jérôme, *Macromolecules*, 1998, **31**, 213; (*e*) S. Jousset, S. O. Hammouch and J.-M. Catala, *Macromolecules*, 1997, **30**, 6685; (*f*) A. Goto, T. Terauchi, T. Fukuda and T. Miyamoto, *Macromol. Rapid Commun.*, 1997, **18**, 673; (*g*) I. Q. Li, B. A. Howell, M. T. Dineen, P. E. Kastl, J. W. Lyons, D. M. Meunier, P. B. Smith and D. B. Priddy, *Macromolecules*, 1997, **30**, 5195; (*h*) S. A. F. Bon, M. Bosveld, B. Klumperman and A. L. German, *Macromolecules*, 1997, **30**, 324; (*i*) R. D. Puts and D. Y. Sogah, *Macromolecules*, 1996, **29**, 3323; (*j*) M. Hölderle, M. Baumert and R. Mülhaupt, *Macromolecules*, 1997, **30**, 3420, and further work of these groups.
2 H. Fischer, *Macromolecules*, 1997, **30**, 5666.
3 (*a*) J. L. Wang, T. T. Grimaud and K. Matyjaszewski, *Macromolecules*, 1997, **30**, 6507; (*b*) V. Percec and B. Barboiu, *Macromolecules*, 1995, **28**, 7970; (*c*) G. Moineau, C. Granel, P. Dubois, R. Jérôme and P. Teyssié, *Macromolecules*, 1998, **31**, 542; (*d*) T. Ando, M. Kato, M. Kamigaito and M. Sawamoto,

Macromolecules, 1996, **29**, 1070; (*e*) B. B. Wayland, L. Basickes, S. Mukerjee, M. Wie and M. Fryd, *Macromolecules*, 1997, **30**, 8108, and further references therein.
4 (*a*) H. Fischer, *J. Am. Chem. Soc.*, 1986, **108**, 3925; (*b*) D. Rüegge and H. Fischer, *Int. J. Chem. Kinet.*, 1989, **21**, 703; (*c*) C. Walling, *J. Am. Chem. Soc.*, 1988, **110**, 6846; (*d*) B. E. Daikh and R. G. Finke, *J. Am. Chem. Soc.*, 1992, **114**, 2938; (*e*) P. A. MacFaul, I. W. C. E. Arens, K. U. Ingold and D. D. M. Wayner, *J. Chem. Soc., Perkin Trans. 2*, 1997, 135; (*f*) A. Bravo, H.-R. Bjorsvik, F. Fontana, L. Liguori and F. Minisci, *J. Org. Chem.*, 1997, **62**, 3849; (*g*) T. Kothe, R. Martschke and H. Fischer, *J. Chem. Soc., Perkin Trans. 2*, 1998, 503.
5 (*a*) J. Chateauneuf, J. Lusztyk and K. U. Ingold, *J. Org. Chem.*, 1988, **53**, 1629; (*b*) A. L. J. Beckwith, V. W. Bowry and G. Moad, *J. Org. Chem.*, 1988, **53**, 1632; (*c*) A. L. J. Beckwith, V. W. Bowry and K. U. Ingold, *J. Am. Chem. Soc.*, 1992, **114**, 4983; (*d*) V. W. Bowry and K. U. Ingold, *J. Am. Chem. Soc.*, 1992, **114**, 4992; (*e*) M. V. Baldovi, N. Mohtat and J. C. Scaiano, *Macromolecules*, 1996, **29**, 5497; (*f*) I. W. C. E. Arends, P. Mulder, K. B. Clark and D. M. Wayner, *J. Phys. Chem.*, 1995, **99**, 8182.
6 S. N. Batchelor, *J. Phys. Chem. B*, 1998, **102**, 615, and personal communication.
7 S. F. Nelsen and P. D. Bartlett, *J. Am. Chem. Soc.*, 1966, **88**, 137; R. C. Neuman, Jr. and M. J. Amrich, Jr., *J. Am. Chem. Soc.*, 1980, **45**, 4629; K. J. Skinner, H. S. Hochster and J. M. McBride, *J. Am. Chem. Soc.*, 1974, **96**, 4301.
8 This solution became first apparent from numerical calculations. An example is seen in Fig. 1 of our early work.[4a]
9 (*a*) T. J. Connolly, M. V. Baldovi, N. Mohtat and J. C. Scaiano, *Tetrahedron Lett.*, 1996, **37**, 4919; (*b*) J. C. Scaiano, M. Tanner and D. Weir, *J. Am. Chem. Soc.*, 1985, **107**, 4396.
10 (*a*) P. D. Bartlett and T. Funahsi, *J. Am. Chem. Soc.*, 1962, **84**, 2596; (*b*) M. S. Kharash and B. S. Joshi, *J. Org. Chem.*, 1957, **22**, 1435.
11 Y. P. Tsentalovich and H. Fischer, *J. Chem. Soc., Perkin Trans. 2*, 1994, 729; M. Salzmann, Y. P. Tsentalovich and H. Fischer, *J. Chem. Soc., Perkin Trans. 2*, 1994, 2119; R. Martschke, R. D. Farley and H. Fischer, *Helv. Chim. Acta*, 1997, **80**, 1363.
12 (*a*) J. K. Vollenweider, H. Fischer, J. Hennig and R. Leuschner, *Chem. Phys.*, 1985, **97**, 217; (*b*) R. Hany and H. Fischer, *Chem. Phys.*, 1993, **172**, 131.
13 J. L. Faria and S. Steenken, *J. Phys. Chem.*, 1992, **96**, 10 869.
14 E. C. Korolenko, F. L. Cozens and J. C. Scaiano, *J. Phys. Chem.*, 1995, **99**, 14 123.
15 (*a*) S. N. Batchelor and H. Fischer, *J. Phys. Chem.*, 1996, **100**, 9794; (*b*) Y. P. Tsentalovich, A. A. Obychochny and R. Z. Sagdeev, *Chem. Phys.*, 1989, **139**, 301; (*c*) T. Aizawa, A. Araki, K. Shindo, K. Maeda and T. Azumi, *Spectrochim. Acta, Part A*, 1994, **50**, 1443.
16 J. A. Howard and J. C. Tait, *J. Org. Chem.*, 1978, **43**, 4279.
17 I. Li, B. A. Howell, K. Matyjaszewski, T. Shigemoto, P. B. Smith and D. P. Priddy, *Macromolecules*, 1995, **28**, 6692.
18 C. J. Hawker, G. G. Barclay, A. Orellana, J. Dao and W. Devonport, *Macromolecules*, 1996, **29**, 5245.
19 T. Fukuda, Y. Tsujii and T. Miyamoto, *Polym. Prepr. (Am. Chem. Soc., Div. Polym. Chem.)*, 1997, **38**, 723.
20 T. Fukuda, T. Terauchi, A. Goto, K. Ohno, Y. Tsujii and B. Yamada, *Macromolecules*, 1996, **29**, 6393; R. P. N. Veregin, P. G. Odell, L. M. Michalak and M. K. Georges, *Macromolecules*, 1996, **29**, 2746; P. J. MacLeod, R. P. N. Veregin, P. G. Odell and M. K. Georges, *Macromolecules*, 1998, **31**, 530.
21 K. Matyjaszewski and A. Kajiwara, *Macromolecules*, 1998, **31**, 548.
22 G. Moad and E. Rizzardo, *Macromolecules*, 1995, **28**, 8722.
23 A. Goto, T. Terauchi, T. Fukuda and T. Miyamoto, *Macromol. Rapid Commun.*, 1997, **18**, 673.
24 P. M. Kazmaier, K. A. Moffat, M. K. Georges, R. P. N. Veregin and G. K. Hamer, *Macromolecules*, 1995, **28**, 1841.